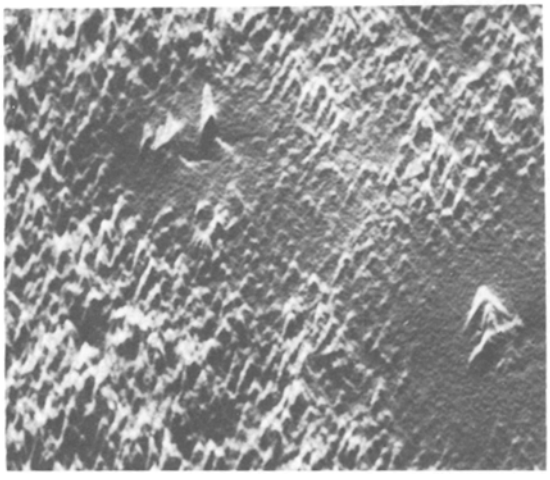

Figure 4 SEM ($Y-Z$, 34° tilt) of the cadmium film showing the initial nucleation stage (× 2800).

References

1. YU F. KOMNIK and E. I. BUKHSHTAB, *JETP Letters* **6** (1967) 58.
2. L. S. PALATNIK and V. M. KOSERICH, *Kristallogr.* **3** (1958) 709.
3. L. S. PALATNIK and YU F. KOMNIK, *Sov. Phys. Doklady* **5** (1960) 1072.

Received 18 October 1978
and accepted 31 May 1979

S. K. BANDYOPADHYAY
A. K. PAL
Department of General Physics and X-rays,
Indian Association for the Cultivation of Science,
Calcutta 700032,
India
G. L. MALHOTRA
National Physical Laboratory
New Delhi,
India

Glass fibres containing metallic granules

Oxide glasses containing dispersed metallic granules of dimensions of the order of a few hundred angstroms show electrical conduction by an electron tunnelling mechanism between the metallic islands [1, 2]. It is therefore likely that electroconducting glass fibres can be made by inducing in them a microstructure similar to the above. There is also the possibility of obtaining glass fibres with improved mechanical properties by this method. In this communication we describe the results obtained on some glass fibres containing a dispersion of metallic particles.

The compositions of glasses used are given in Table I. These were arrived at by a trial and error method to ensure the twin requirements of proper microstructure and the liquidus temperature versus viscosity relation necessary for continuous fiberizing. The glasses were prepared from reagent-grade chemicals in 100 g batches. Ag_2O and B_2O_3 were introduced in the form of Ag_2SO_4 and H_3BO_3, respectively, and the rest of the components as their oxides. The mixtures were at first heated slowly in the range 600 to 1100° C in high-density alumina crucibles in an electrically heated furnace. The final melting was carried out in the range 1300 to 1400° C for a period of $\frac{1}{2}$ h. This schedule was followed to ensure a homogeneous glass with less loss of Ag_2O [3]. The molten glass was cast in an aluminium mould. Glass frit obtained was remelted and fiberized using a single-orifice bushing made of pure alumina [4] which was mounted in a furnace having silicon carbide rods as heating elements. A typical fiberization temperature was ~ 1100° C. Continuous glass filaments were drawn onto a rotating drum at a surface speed of 4500 ft min^{-1}. The diameters of the glass fibres obtained varied between 10 and 12 μm. Fibres drawn from glasses 2, 3 and 4, respectively, have a microstructure consisting of metallic silver and/or bismuth particles (depending on the starting composition) of diameters ranging from 100 to 500 Å dispersed in a glass matrix. A typical transmission electron

TABLE I Compositions of glasses (mol %) for drawing fibres

Glass no.	SiO_2	B_2O_3	K_2O	Al_2O_3	As_2O_3	Bi_2O_3	Ag_2O
1	46	28	11	9	2	0	0
2	46	25	11	9	1	0	4
3	46	23	11	9	2	0	6
4	51	25	11	5	1	3	4

0022–2461/79/122991–04$02.40/0

micrograph for a fibre sample of glass 3 is shown in Fig. 1.

The tensile strengths and Young's moduli of the glass fibres of different compositions were measured by an Instron machine operating at a cross-head speed of 0.02 cm min^{-1}. A gauge length of 50 mm was used for all the fibres. At least ten fibres of each glass were tested to compute the average values which are given in Table II. It is seen from this table that there is a small improvement in the strength values in fibres of compositions 3 and 4, respectively. This could arise due to the deflection of microcracks along the glass/metal interface during the course of its propagation [5]. However, more detailed studies are necessary before any conclusion can be drawn. All the fibres containing metallic particles show higher values of Young's modulus than that of the base glass fibre. This is believed to be due to the higher modulus of silver. Using the rule of mixtures [6] and the volume fractions of the metallic phase in the different glasses as determined from the electron micrographs [7], the composite Young's modulus values were calculated and are shown in the last column of Table II. These are in reasonable agreement with the experimental values.

D.c. conductivity of the fibres was measured by mounting bundles of 50 fibres with a length of 1.5 cm in a specially constructed sample holder using silver paint as electrodes at each end [8]. Measurements of voltage–current characteristics over a decade of voltage were carried out in the temperature range 30 to 350° C using an ECIL Picoammeter EA813B. Linearity of the I–V curves was obtained for all specimens and the resistances were calculated from their slopes.

The d.c. resistivity data are shown in Fig. 2. The activation energy of 0.6 eV as obtained for glass 1 is evidently due to the migration of potassium ions through the glass [9]. In the case of glasses containing metallic species, however, the slope decreases at temperatures lower than 200° C. This behaviour arises due to electron tunnelling between metallic islands [1, 2]. It has been shown [11] that for low electric fields the resistivity of granular metals when the particles are isolated from each other is given by,

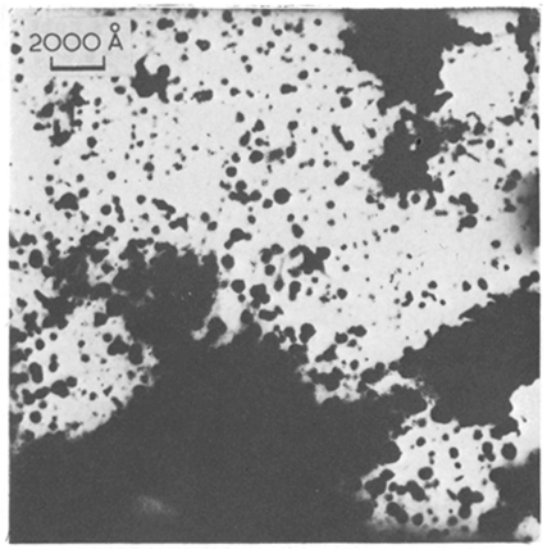

Figure 1 Transmission electron micrograph of fibre from glass 3.

$$\rho = \rho_0 \exp\left[2\left(\frac{C}{KT}\right)^{1/2}\right]. \quad (1)$$

In this equation, ρ_0 can be assumed to be constant to a first order approximation and

$$C = \chi s E_c^0, \quad (2)$$

where

$$\chi = \left[\frac{2m\phi}{\hbar^2}\right]^{1/2}, \quad (3)$$

TABLE II Tensile strength and Young's modulus for glass fibres of different compositions

Glass no.	Tensile strength (psi × 10^{-5})*	Young's modulus (psi × 10^{-6})	Volume fraction of metal phase	Calculated Young's modulus from mixture rule (psi × 10^{-6})
1	1.1 ± 0.2	7.7 ± 0.3	–	–
2	1.1 ± 0.2	9.3 ± 0.3	0.20	8.4
3	1.7 ± 0.3	8.0 ± 0.6	0.33	8.8
4	1.3 ± 0.1	9.8 ± 0.3	0.22	8.5

* 10^3 psi ≡ 6.89 N mm^{-2}.

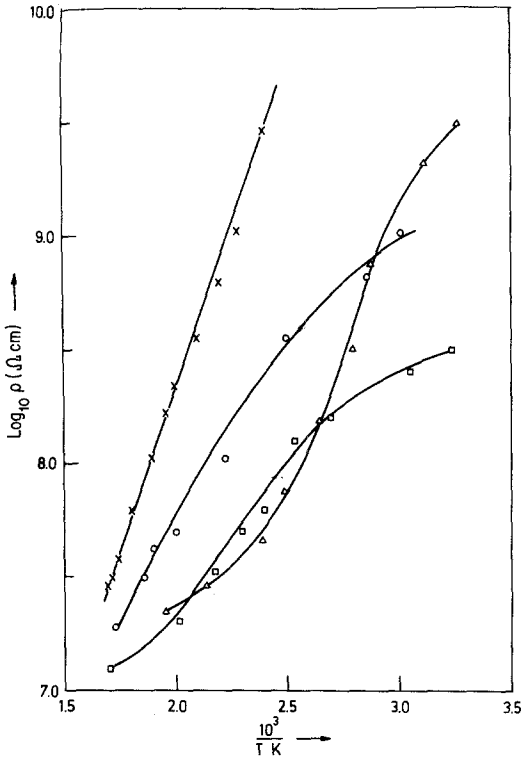

Figure 2 Resistivity–temperature plots for fibres from different glasses. x Glass 1, ○ glass 2, □ glass 3, △ glass 4.

with m denoting the electron mass, ϕ the effective barrier height, and $\hbar$ Planck's constant; s is the separation between the grains, E_c^0 is the energy required to generate a pair of fully dissociated positively and negatively charged grains and is given by,

$$E_c^0 = \frac{2e^2}{Kd}, \tag{4}$$

where

$$K = \epsilon[1 + (d/2s)], \tag{5}$$

ϵ being the dielectric constant of the insulating medium and d the grain size.

TABLE III Electron tunnelling parameters for glass fibres with metallic dispersion

Glass no.	C (eV)	E_c^0 (eV)	d (Å)	E_c^0 (calc.) (eV)
2	5.2	1.7×10^{-2}	500	2.2×10^{-2}
3	3.6	8.4×10^{-3}	430	1.5×10^{-2}
4	2.6	2.0×10^{-3}	130	6.5×10^{-2}

E_c^0: energy of formation of a pair of positively and negatively charged grains.
d: average diameter of metallic grains.

TABLE IV Calculated and experimental resistivity values of different glass fibres at 307° C

Glass no.	V_f	ρ_{exp} (Ω cm)	ρ_{calc} (Ω cm)
2	0.20	1.9×10^7	1.9×10^7
3	0.33	1.3×10^7	1.4×10^7
4	0.22	1.8×10^7	1.8×10^7

The d.c. resistivity data were therefore plotted as $\log \rho$ versus $1/T^{1/2}$. The curves were found to be linear and C values for different glasses were calculated from their slopes. Taking $\chi = 1\,\text{Å}^{-1}$ [1] and $s \sim 50$ Å, values of E_c^0 were estimated from Equation 2. The results are given in Table III. Values of E_c^0 were also calculated from Equation 5 by taking $\epsilon = 4$ [1] and suitable values of d as found from the micrographs of the different glasses containing metallic granules. These are also shown in Table III. The experimental and calculated values of E_c^0 are in reasonable agreement confirming the electron tunnelling mechanism of conduction in the present system.

At higher temperatures, the glass fibres containing metallic granules show lower resistivity values than those of fibres drawn from the base glass composition. This can be explained as follows. For a composite consisting of a randomly distributed spherical particles of resistivity ρ_s in a matrix of resistivity ρ_m such that $\rho_s \ll \rho_m$, the resistivity of the system ρ_c is given by [10]

$$\rho_c \simeq \rho_m \frac{1 - V_f}{1 + 2V_f} \tag{6}$$

where V_f is the volume fraction of the dispersed phase. Using this equation, the resistivity values at 307° C for different fibres were calculated. The results are given in Table IV. The calculated values are in excellent agreement with the experimental data.

References

1. D. CHAKRAVORTY, A. K. BANDYOPADHYAY and V. K. NAGESH, *J. Phys. D. Appl. Phys.* **10** (1977) 2077.
2. D. CHAKRAVORTY, A. R. HARANAHALLI and D. KUMAR, *Phys. Stat. Sol.* (a) **51** (1979) 275.
3. E. F. RIEBLING, *J. Chem. Phys.* **55** (1971) 804.
4. D. CHAKRAVORTY and R. BHATNAGAR, Proceedings of the International Symposium on Fibres and Composites, New Delhi. Vol. 1 (1976) p. 7.1.

5. P. HING and P. W. McMILLAN, *J. Mater. Sci.* 8 (1973) 1041.
6. L. J. BROUTMAN and R. H. KROCK, "Modern Composite Materials" (Addison-Wesley, Reading, MA, USA, 1976) p. 13.
7. R. T. DEHOFF and F. N. RHINES, "Quantitative Microscopy" (McGraw-Hill, New York, 1968).
8. J. D. PROVANCE and J. S. HUEBNER, *J. Amer. Ceram. Soc.* 54 (1971) 147.
9. J. M. STEVELS, "Handbuch der Physik", Vol. XX, edited by S. W. Flugge (Springer-Verlag, Berlin, 1957) p. 350.
10. E. H. KERNER, *Proc. Phys. Soc. London* B69 (1956) 802.
11. B. ABELES, SHENG PING, M. D. COUTTS and Y. ARIE, *Adv. Phys.* 24 (1975) 407.

Received 28 February
and accepted 10 May 1979

D. CHAKRAVORTY
B. N. KESHAVARAM
A. VENKATESWARAN
Materials Science Programme,
Indian Institute of Technology,
Kanpur, India

The lowest laser–Raman active accordion (ALR) type oscillations in crystalline polymers

The longitudinal accordion-type mode (LAM) frequencies of crystals of linear polymers with the chains perpendicular to the lamella surface are imagined as corresponding to the longitudinal eigenfrequencies of an ideally elastic rod of length D having the maximum amplitude at its ends. In such a case the eigenmodes have a wavelength $\lambda = 2D, 2D/2, 2D/3 \ldots$. Among them only those corresponding to $\lambda_1, \lambda_3 \ldots$ having a node in the centre of the rod are Raman active. They can be labelled ALR1, ALR2,... since only these wavelengths λ_{Rn}, frequencies $\nu_{Rn} = c_{ac}/\lambda_{Rn}$ or wave numbers ν^*_{Rn}/c_{opt} are observed in the laser-Raman scattering experiment. Here $c_{ac} = (E/\rho)^{1/2}$ is the sound velocity and $c_{opt} = 3 \times 10^8$ m sec^{-1} is the light velocity. The ratio of the corresponding eigenfrequencies or wave numbers is expected to be 1:3:5:.... Small deviations can be easily attributed to end groups, chain folds, strong repulsive forces, and similar small effects which shift the eigenfrequencies of the elastic rod to a lower value if they contribute a mass, and to a higher value if they contribute an additional restoring force.

The experiments agree to a large extent with this view if one is concerned with linear polymers having a zig-zag conformation in the crystal lattice and, hence, a very high axial elastic modulus. Strobl and Eckel [1] report on linear polyethylene (PE) wave number values $\nu^*_{R1} = 24.2 \pm 0.3$ cm^{-1} and $\nu^*_{R2} = 69.0 \pm 1$ cm^{-1}. Their ratio is 2.85 which is so close to 3 that one does not worry too much about the model. The situation deteriorates a little if one considers the true maxima of polarizability derivatives which according to Krimm and Hsu [2] shifts the ALR1 wave number to 24.9 ± 0.3 cm^{-1} thus yielding for the ratio of the second to the first accordion-type Raman frequencies the value, 2.77 which is a little further away from 3 than 2.85.

The situation is much less satisfactory with polymers which crystallize with the chains in helical conformation, as for instance polypropylene (PP) [3], polyoxymethylene (POM) [4], and poly(ethylene oxide) (POE) [5]. The ALR1 wave numbers differ so much from those calculated for independent elastic rods with the known density ρ_c and elastic modulus E_c that one has to consider the addition of restoring forces at the ends of the crystalline rods [6] or the coupling of rods through the amorphous layers [6, 7]. It turned out that the model of coupled rods reproduces the data in a simpler manner and in better agreement with the physics of the system [7].

The first and second ALR scattering wave numbers were measured on PEO. Shepherd and coworkers [8–10] report $\nu^*_{R1} = 9.2 \pm 0.3$ cm and $\nu^*_{R2} = 19.0 \pm 1$ cm^{-1} with the ratio 2.06 which differs so much from 3 that it is certain that something must be wrong with the model. The situation becomes still more extreme if one calculates the true maxima of polarizability derivative which, according to Krimm and Hsu [2], shifts the wave number ν^*_{R1} by 10% and that of ν^*_{R2} by 3% to higher values. With the so-corrected values, $\nu^*_{R1} = 10.12 \pm 0.3$ cm^{-1} and $\nu^*_{R2} = 19.57 \pm 1$ cm^{-1}, one has the ratio $\nu^*_{R2}/\nu^*_{R1} = 1.93 \pm 0.15$ which is even lower than 2.

 0022–2461/79/122994–05$02.50/0